Multi Hypothesis Track Extraction and Maintenance of GMTI Sensor Data

Jost Koller
FGAN-FKIE
Neuenahrer Strasse 20
D-53343 Wachtberg, Germany
koller@fgan.de

Martin Ulmke
FGAN-FKIE
Neuenahrer Strasse 20
D-53343 Wachtberg, Germany
ulmke@fgan.de

Abstract – *This contribution presents an application of a multi hypothesis tracking (MHT) algorithm to the case of ground moving targets detected by GMTI (Ground Moving Target Indicator) sensors. We describe in some detail how the following tracking tasks are performed: track extraction, prediction, filtering, track maintenance and retrodiction (smoothing). The experimental implementation has been successfully tested in a NC3A (NATO Consultation, Command and Control Agency) testbed with simulated GMTI data of various ground surveillance sensors. Ongoing developments and improvements are discussed.*

Keywords: STAP (Space Time Adaptive Processing), GMTI (Ground Moving Target Indicator), GMTI tracking, MHT (Multiple Hypothesis Tracking), Sequential Track Extraction

1 INTRODUCTION

In modern military conflicts, capabilities for long-range and near real-time ground surveillance are increasingly required. One important sensor technology for such a task is airborne GMTI radar with STAP processing [1], which already is or will be soon available from a number of different platforms. The purpose of automatic target tracking is to facilitate surveillance by providing continuous high quality tracks of single vehicles and military equipment as well as aggregations such as convoys. Ground target tracking with airborne sensors often suffers from low visibility, high clutter and high target density. The use of modern tracking algorithms for many targets in a cluttered environment therefore is indispensable in order to obtain sensible results. Furthermore, the exploitation of as much a priori information as possible on the sensor as well as on the targets and, in particular, on the terrain is suitable to enhance track quality and track continuity.

The increasing interest in aerial ground surveillance is reflected in the formation of international technology projects for joint airborne ground surveillance. The purpose of such projects is to establish interoperability by integrating, exploiting, and sharing sensor data from different surveillance platforms to the associated ground stations. Relevant sensor types in this context are predominantly GMTI and synthetic aperture radar (SAR) but in future also optical, infrared, and electronic intelligence (ELINT) sensors.

There exist different national exploitation stations for aerial ground surveillance. In Germany an experimental "Interoperable Image Exploitation Station" (IIES) is in developement, lead by EADS, Defence and Communications Systems. One current task is the integration of an experimental interactive tracking component. An important objective of such technology programs are exercises (simulated or real) to evaluate program technology and operational concepts. Such real data as well as realistically simulated MTI sensor data are extremely valuable for a reliable evaluation of different tracking algorithms.

In the following we present an application of a multi hypothesis tracking (MHT) algorithm to the case of ground moving targets detected by GMTI (Ground Moving Target Indicator) sensors. The paper is is organized as follows: Section 2 decribes the elements of the BAYESian MHT algorithm, including track extraction, prediction, filtering, track maintenance and retrodiction, and the modifications necessary for the processing of GMTI-sensor data. Experimental results for simulated MTI sensor data will be presented in Section 3.

2 Multi Hypothesis Tracking

In general, BAYESian tracking algorithms perform sequential updates of the probability density function (pdf), $p(\mathbf{x}_k|Z^k)$, of a target state $\mathbf{x}_k$ at time t_k, conditioned on the incoming measurements up to that time Z^k.[2, 3] Here, Z^k denotes all measurements of each scan up to the $k-$th scan, i.e. $Z^k = \{Z_1, Z_2, \ldots, Z_k\}$.

Multiple hypothesis tracking (MHT) consists of several tasks: target track extraction, prediction, filtering, track

maintenance, and retrodiction. In this section, we describe in some detail how each of these tasks is realized.

2.1 Dynamical Model and Kalman Filtering

The dynamical model is chosen and adapted to ground moving targets. Since these targets typically exhibit much less agility than military air targets, the inclusion of accelerations into the state vector may not be necessary. Therefore the target state at time t_k is defined by

$$\mathbf{x}_k = (\mathbf{r}_k\ \dot{\mathbf{r}}_k)^\top = (x_{k;1}\ \cdots\ x_{k;6})^\top$$

Under idealized circumstances, one may set the z-coordinates $x_{k;3} = x_{k;6} = 0$. The probabilities of the hypotheses representing a target are dependent on the algorithm used for data processing, and the underlying target dynamics model. The Kalman filter assumes that the posterior density at every time step is Gaussian, i.e. completely described by its mean and covariance. The filtered probability density $p(\mathbf{x}_{k+1}|\mathbf{Z}^{k+1})$ is Gaussian as well, implying the following assumptions: As widely accepted in the tracking literature [2], the underlying dynamical model is a known linear Markov process:

$$\mathbf{x}_{k+1} = \mathbf{F}_{k+1|k}\mathbf{x}_k + \mathbf{G}_{k+1|k}\mathbf{v}_{k+1} \tag{1}$$

and the measurement is a linear function of the target state:

$$\mathbf{z}_k = \mathbf{H}_k\mathbf{x}_k + \mathbf{w}_k, \tag{2}$$

with Gaussian process and measurement noise, $\mathbf{v}_k$ and $\mathbf{w}_k$, resp.. Following the realization of [4], the matrices $\mathbf{F}_{k+1|k}$ and $\mathbf{G}_{k+1|k}$ are given by

$$\mathbf{F}_{k+1|k} = \begin{pmatrix} \mathbf{J} & t_{k+1|k}\mathbf{J} \\ \mathbf{0} & \mathrm{e}^{-t_{k+1|k}/\theta_t}\mathbf{J} \end{pmatrix} \tag{3}$$

and

$$\mathbf{G}_{k+1|k} = \Sigma_{k+1|k} \begin{pmatrix} \mathbf{0} \\ \mathbf{J} \end{pmatrix}.$$

with

$$t_{k+1|k} = t_{k+1} - t_k, \quad \Sigma_{k+1|k} = v_t\sqrt{1 - \mathrm{e}^{-2t_{k+1|k}/\theta_t}}, \tag{4}$$

and $\mathbf{J} = \mathrm{diag}[1, 1, 0]$ and $\mathbf{0} = \mathrm{diag}[0, 0, 0]$. It can be shown that the modeled target velocity is ergodic and given by

$$\mathbb{E}[\dot{\mathbf{r}}_k] = 0, \quad \mathbb{E}[\dot{\mathbf{r}}_k\dot{\mathbf{r}}_l^\top] = v_t^2\mathrm{e}^{-2(k-l)t_{k+1|k}/\theta_t}.$$

The parameter v_t means a velocity limitation, and θ_t is called maneuver correlation time. Both parameters have to be chosen appropriately.

The filtering of the hypotheses is carried out within the well known Kalman formalism. Since our target dynamics are based on coordinate uncoupled maneuvers [5], the Kalman filter are uncoupled in x and y as well. The estimated target state in the k-th scan is described by a normal mixture of $\hat{n}_k$ individual track hypotheses,

$$\begin{aligned} p(\mathbf{x}_k|Z^k) &= \sum_{i=1}^{\hat{n}_k} p^i(\mathbf{x}_k|Z^k) \\ &= \sum_{i=1}^{\hat{n}_k} p_k^i\ \mathcal{N}(\mathbf{x}_k;\ \hat{\mathbf{x}}_{k|k}^i,\ \mathbf{P}_{k|k}^i). \end{aligned} \tag{5}$$

(See [6] for the definition of the normal distribution $\mathcal{N}$.) Thus Z_k is the set of the n_k measurements in the $k-$th scan: $Z_k = \{\mathbf{z}_k^1, \mathbf{z}_k^2, \ldots, \mathbf{z}_k^{n_k}\}$. As will be shown later, the number of measurements n_k and hypotheses $\hat{n}_k$ normally differ. The individual weights p_k^i have to fulfill the condition $\sum_i p_k^i = 1$.

Applying the Bayes rule and the Markov property (1), the predicted probability densities for each hypothesis at the time t_{k+1} are given by

$$p^i(\mathbf{x}_{k+1}|Z^k) = \int p(\mathbf{x}_{k+1}|\mathbf{x}_k)p^i(\mathbf{x}_k|Z^k)\ d\mathbf{x}_k \tag{6}$$

Evaluation of Eq. (6) again yields a normal mixture analogue to Eq. (5) but with means $\mathbf{x}_{k+1|k}^i$ and covariances $\mathbf{P}_{k+1|k}^i$, which can be calculated by

$$\begin{aligned} \hat{\mathbf{x}}_{k+1|k}^i &= \mathbf{F}_{k+1|k}\ \hat{\mathbf{x}}_{k|k}^i \\ \mathbf{P}_{k+1|k}^i &= \mathbf{F}_{k+1|k}\mathbf{P}_{k|k}^i\mathbf{F}_{k+1|k}^\top + \mathbf{G}_{k+1|k}\mathbf{G}_{k+1|k}^\top. \end{aligned}$$

Each predicted hypothesis i now is evaluated with each incoming measurement $\mathbf{z}^j$ using the Bayes formalism,

$$p^{ij}(\mathbf{x}_{k+1}|Z^{k+1}) \propto p(\mathbf{z}_{k+1}^j|\mathbf{x}_{k+1})\ p^i(\mathbf{x}_{k+1}|Z^k),$$

where $p^i(\mathbf{x}_{k+1}|Z^k)$ is the predicted probability density function (pdf) from Eq. (6) and $p(\mathbf{z}_{k+1}^j|\mathbf{x}_{k+1})$ is the likelihood function for the j-th measurements given the target position. Assuming $\mathbf{w}_k$ in Eq. (2) to be Gaussian, the likelihood function is normal and given by

$$p(\mathbf{z}_{k+1}^j|\mathbf{x}_{k+1}) = \mathcal{N}(\mathbf{z}_{k+1}^j; \mathbf{H}_k\mathbf{x}_{k+1}, \mathbf{R}_k)$$

with the covariance $\mathbf{R}_k = \mathbb{E}[\mathbf{w}_k\mathbf{w}_k^\top]$ of the measurement noise vector. In multi hypothesis tracking, one has to account for the case, that the target has not been detected, i.e. all measurements are false alarms. Supposing there are n_{k+1} measurements at time t_k, the MHT likelihood function for the measurement set is given by:

$$\begin{aligned} p(Z_{k+1}|\mathbf{x}_{k+1}) &\propto (1 - P_d)f_c + \\ &+ P_d\sum_{j=1}^{n_{k+1}} \mathcal{N}(\mathbf{z}_{k+1}^j; \mathbf{H}_k\mathbf{x}_{k+1}, \mathbf{R}^j), \end{aligned} \tag{8}$$

where f_c denotes the clutter density and P_d the target detection probability. The pdf of the estimated target state

after the update with the new measurements is calculated by further application of the Bayes theorem. In the following result, the index $j = 0$ expresses the hypothesis of not detecting the target (i.e. the first part of the right hand side of Eq. (8)):

$$p(\mathbf{x}_{k+1}|Z^{k+1}) = \sum_{i=1}^{\hat{n}_k} \sum_{j=0}^{n_{k+1}} p_{k+1}^{ij} \mathcal{N}(\mathbf{x}_{k+1};\, \hat{\mathbf{x}}_{k+1|k+1}^{ij},\, \mathbf{P}_{k+1|k+1}^{ij}), \tag{9}$$

To determine the hypotheses weights p_{k+1}^{ij}, calculate the preliminary hypotheses weights $\hat{p}_{k+1}^{ij}$

$$\hat{p}_{k+1}^{ij} = \begin{cases} p_k^i \frac{P_d}{f_c} \mathcal{N}(\mathbf{z}_{k+1}^j;\, \mathbf{H}_{k+1}\hat{\mathbf{x}}_{k+1|k}^i,\, \mathbf{H}_{k+1}\mathbf{P}_{k+1|k}^i\mathbf{H}_{k+1}^\top + \mathbf{R}_k^j) \\ \qquad \text{if } j > 0 \\ p_k^i(1 - P_d), \quad \text{if } j = 0\,. \end{cases} \tag{10}$$

To ensure the completeness of the multi-hypothesis approach, the coefficients $\hat{p}_{k+1}^{ij}$ have to be normalized to unity, i.e.

$$p_{k+1}^{ij} = \frac{\hat{p}_{k+1}^{ij}}{\sum_{i=1}^{\hat{n}_k} \sum_{j=0}^{n_{k+1}} \hat{p}_{k+1}^{ij}} \tag{11}$$

Equation (9) may be re-indexed to achieve the same formal structure as Eq. (5), but with $\hat{n}_{k+1} = \hat{n}_k(n_{k+1} + 1)$ hypotheses. The means and covariances are computed as follows:

$$\begin{aligned} \hat{\mathbf{x}}_{k+1|k+1}^{ij} &= \hat{\mathbf{x}}_{k|k}^i + \mathbf{K}_{k+1}(\mathbf{z}_{k+1}^j - \mathbf{H}_{k+1}\hat{\mathbf{x}}_{k+1|k}^i) \\ \mathbf{P}_{k+1|k+1}^{ij} &= \mathbf{P}_{k+1|k}^i - \mathbf{K}_{k+1}^{ij}\mathbf{S}_{k+1}^{ij}\mathbf{K}_{k+1}^{ij^\top}\,. \end{aligned}$$

with Kalman gain $\mathbf{K}_{k+1}^{ij}$ and innovation covariance $\mathbf{S}_k^{ij}$

$$\begin{aligned} \mathbf{K}_{k+1}^{ij} &= \mathbf{P}_{k+1|k}^i \mathbf{H}_{k+1}^\top \mathbf{S}_{k+1}^{ij} \\ \mathbf{S}_{k+1}^{ij} &= \mathbf{H}_{k+1}\mathbf{P}_{k+1|k}^i \mathbf{H}_{k+1}^\top + \mathbf{R}_k^j \end{aligned}$$

2.2 Hypotheses Reduction

As it is obvious from Eq. (9), the number of hypotheses increases dramatically from scan to scan because of the combinatorial disaster, i.e. $\hat{n}_{k+1} = \hat{n}_k(n_{k+1} + 1)$. To diminish the number of hypotheses, we use several techniques. The first technique is individual *gating* when assigning the measurements to the predicted hypotheses. The predicted covariance of each hypothesis together with the measurement error covariance forms an expectation area (gate), and only measurements inside this gate, defined by

$$\left(\mathbf{z}_{k+1}^j - \mathbf{H}_{k+1}\hat{\mathbf{x}}_{k+1|k}^i\right)^\top \left(\mathbf{S}_{k+1}^{ij}\right)^{-1} \left(\mathbf{z}_{k+1}^j - \mathbf{H}_{k+1}\hat{\mathbf{x}}_{k+1|k}^i\right) < \lambda^2$$

are used to build up the hypothesis to the considered hypothesis. The parameter λ is chosen empirically as 13.8. The next step to reduce the number of hypotheses is *pruning*, which means the deletion of all hypotheses with weight p_k^i smaller than an appropriate threshold, called cut-off-parameter c_{coff}. In our case, we chose $c_{\text{coff}} = 0.001$.
Another way to reduce the number of hypotheses is *merging* of similar hypotheses of a given track. If two hypotheses i and j have very similar state vectors $\hat{\mathbf{x}}_{k|k}^{i/j}$ and covariances $\mathbf{P}_{k|k}^{i/j}$, they are merged into one hypothesis using second moment matching, i.e.

$$\begin{aligned} \hat{\mathbf{x}}_{k|k}^{\text{comb}} &= \sum_{l=i,j} p_k^l \hat{\mathbf{x}}_{k|k}^l \\ \mathbf{P}_{k|k}^{\text{comb}} &= \sum_{l=i,j} p_k^l \left\{ \mathbf{P}_{k|k}^l + \left(\hat{\mathbf{x}}_{k|k}^l - \hat{\mathbf{x}}_{k|k}^{\text{comb}}\right) \cdot \right. \\ &\qquad \left. \cdot \left(\hat{\mathbf{x}}_{k|k}^l - \hat{\mathbf{x}}_{k|k}^{\text{comb}}\right)^\top \right\} \\ p_k^{\text{comb}} &= \sum_{l=i,j} p_k^l\,. \end{aligned}$$

The similarity is detected by a χ^2-test, which is applied to the distance of the state vectors $\hat{\mathbf{x}}_{k|k}^{i/j}$, i.e. the test includes location and velocity of the considered hypotheses. Moreover, the covariances $\mathbf{P}_{k|k}^{i/j}$ must not differ by more than 30 percent, if merging shall be applied.

2.3 Sequential Track Extraction

An important task in target tracking is track extraction. We use a sequential likelihood ratio test [4], which is closely related to the sequential hypothesis testing by Wald [7], and shall be described in some detail. Every measurement at any scan initiates its own extraction process by associating it to measurements in the subsequent scans and building up the list Z^k (see Figure 1).

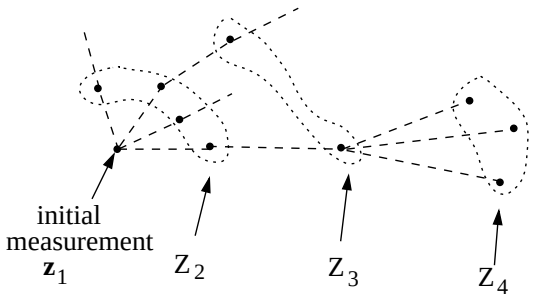

Figure 1: Track extraction starting from an initial measurement

Given a sequence of measurements $Z^k = \{\mathbf{z}_1, Z_2, \ldots, Z_k\}$ arising from one initial measurement $\mathbf{z}_1$, we consider two hypotheses

$\mathcal{H}_0$: the data Z^k contain only false data
$\mathcal{H}_1$: the data Z^k contain target measurements and false alarms

The system, in which the decision has to be made is characterized by the states $\mathbf{z} \in \chi_0$ or $\mathbf{z} \in \chi_1$ where χ_0

denotes the subspace of measurements containing false alarms, only, and χ_1 denotes the supplement. We introduce a cost function for the possible decisions:

$$L(Z^k \in \chi_i | \mathcal{H}_i) = 0 \text{ for } i \in \{0,1\} \quad \text{correct decision}$$
$$L(Z^k \in \chi_i | \mathcal{H}_j) \neq 0 \text{ for } i \in \{0,1\}, i \neq j \quad \text{wrong decision}$$

Minimizing the costs amounts to the calculation of the likelihood ratio and, with the introduction of two thresholds A and B, our sequential likelihood test is defined by

- If

$$L(Z^k) = \frac{p(Z^k|\mathcal{H}_1)}{p(Z^k|\mathcal{H}_0)} \leq B \quad \longrightarrow \quad \text{choose } \mathcal{H}_0 \qquad (15)$$

- If

$$L(Z^k) = \frac{p(Z^k|\mathcal{H}_1)}{p(Z^k|\mathcal{H}_0)} \geq A \quad \longrightarrow \quad \text{choose } \mathcal{H}_1 \qquad (16)$$

- otherwise wait for the next scan and repeat the test.

To derive approximate expressions for A and B, consider the situation where the test terminates. If Eq. (16) terminates, we have

$$p(Z^k|\mathcal{H}_1) \quad \simeq \quad A\, p(Z^k|\mathcal{H}_0)$$

Integrating both sides over χ_1, we obtain

$$P_1 \simeq A P_0 \quad \Longrightarrow \quad A \simeq \frac{P_1}{P_0}$$

where

$$P_1 = \int_{\chi_1} p(Z^k|\mathcal{H}_1)\, dZ^k = \text{Prob.}[\underbrace{\text{accept } \mathcal{H}_1|\mathcal{H}_1}_{\Rightarrow\text{correct decision}}]$$

$$P_0 = \int_{\chi_1} p(Z^k|\mathcal{H}_0)\, dZ^k = \text{Prob.}[\underbrace{\text{accept } \mathcal{H}_1|\mathcal{H}_0}_{\Rightarrow\text{wrong decision}}]$$

In the same way consider the case where the sequential test terminates because of $L(Z^k) \leq B$. Integrating Eq. (15) over χ_0 leads to

$$\int_{\chi_0} p(Z^k|\mathcal{H}_1)\, dZ^k \quad = \quad 1 - \underbrace{\int_{\chi_1} p(Z^k|\mathcal{H}_1)\, dZ^k}_{=P_1} \simeq$$

$$B \int_{\chi_0} p(Z^k|\mathcal{H}_0)\, dZ^k \quad = \quad B \left(1 - \underbrace{\int_{\chi_1} p(Z^k|\mathcal{H}_0)\, dZ^k}_{=P_0} \right)$$

or

$$B \simeq \frac{1 - P_1}{1 - P_0} \,.$$

The track detection probabilities must be chosen reasonably, i.e. $P_1 = 0.95...0.99$ and the false-track probability $P_0 = 0.001...0.01$. It can be shown that the desired likelihood ratio is given by the sum of all unnormalized hypothesis weights $\hat{p}_k^i$ from Eq. (10) belonging to one initial measurement, whose hypothesis weight is set to unity, i.e. $\hat{p}_k^1 = 1$

$$L(Z^k) = \sum_{i=1}^{\hat{n}_k} \hat{p}_k^i$$

Once a track is extracted, i.e. the sequential likelihood ratio test terminates because of $L(Z^k) \geq A$, the normal tracking process starts. Therefore the sum of the hypotheses weights will be normalized to unity (see Eq. (11)) and all hypotheses reduction methods shown above will be applied. The number of scans required to extract a target, i.e. the test length depends on the chosen values of A and B, e.g. the higher the probability to make a "correct decision", the longer the test needs.

Furthermore, the sequential likelihood ratio test shown above also is applied on existing tracks for track confirmation. If the regarded target is still detected, the measurements will be correlated and the sequential track extraction will terminate with $L(Z^k) \geq A$ every few scans. Then $\hat{p}$ will normalized and the test starts again. However, if the sequential test procedure terminates with $L(Z^k) \leq B$, track loss is detected and the track is deleted.

2.4 Track Management

Since every measurements starts an extraction process, the sequential extraction test above continously extracts the same track. Therefore, each newly extracted track needs to be checked if it represents a new target or one that is already tracked. In the latter case, the new track has to be deleted, the older track "survives". Besides the track loss detection mentioned above, we have to keep in mind two significant track events, which have to be treated adequately: track *splitting*, and track *converging*. Track splitting happens if a track consists of at least two unresolved targets, and if at least one target departs from the other(s) (see Figure 2). In that case, the tracking program has to start a new track with the separated sub track.

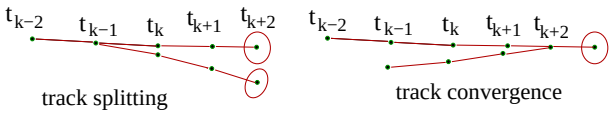

Figure 2: track management for splitting and converging events

The opposite event, track convergence, has to be addressed, too. This may happen if two or more tracks come so close

that they form an unresolved single track. The tracking system has to merge this two tracks, each of them represented by a number of hypotheses, to a single track. Track convergence is much more likely than track splitting since it may happen whenever a false track in the neighborhood of a true target track is fed with the true track data.

2.5 Track Smoothing

The benefits of retrodiction for target tracking are well known and shall be described only shortly. Retrodiction means re-calculation of the track history with the measurements up to the presence, i.e.

$$p(\mathbf{x}_l|Z^l) \xrightarrow{\{Z_{l+1},\ldots,Z^k\}} p(\mathbf{x}_l|Z^k) \quad \text{with} \qquad l < k\,.$$

The Bayes theorem yields

$$p(\mathbf{x}_l|Z^k) = \int \frac{p(\mathbf{x}_{l+1}|\mathbf{x}_l)p(\mathbf{x}_l|Z^l)p(\mathbf{x}_{l+1}|Z^l)}{\int p(\mathbf{x}_{l+1}|\mathbf{x}_l)p(\mathbf{x}_l|Z^l)d\mathbf{x}_l} d\mathbf{x}_{l+1}\,. \quad (18)$$

Evaluation of Eq. (18) provides Kalman like backward iteration formulas

$$\begin{aligned}
\hat{\mathbf{x}}^i_{l|k} &= \hat{\mathbf{x}}^i_{l|l} + \mathbf{W}^i_{l|l+1}\left(\hat{\mathbf{x}}^i_{l+1|k} - \hat{\mathbf{x}}^i_{l+1|l}\right)\\
\mathbf{P}^i_{l|k} &= \mathbf{P}^i_{l|l} + \mathbf{W}^i_{l|l+1}\left(\mathbf{P}^i_{l+1|k} - \mathbf{P}^i_{l+1|l}\right)\mathbf{W}^{i^\top}_{l|l+1}\\
\mathbf{W}^i_{l|l+1} &= \mathbf{P}^i_{l|l}\mathbf{F}^\top_{l+1|l}\mathbf{P}^{i^{-1}}_{l|l}\,.
\end{aligned}$$

with Kalman gain $\mathbf{F}_{l+1|l}$ from Eq. (3). Not only the estimations of state and covariance, but also the hypotheses weights are recalculated. At a given track history, the weight of a hypotheses in the past is re-determined from the weights of its associated hypotheses in the following scan:

$$p^i_l = \sum_{j=1}^{n_{l+1}} p^{ij}_{l+1}$$

where j sums over all hypotheses derived from the $i-$th hypothesis in the $l-$th scan. Due to this recalculation of hypotheses weights, the hypotheses with the highest weight may switch as illustrated in Figure 3. Since this retrodiction induced switching event occurs quite frequently, it is necessary to redraw the subtrack with highest weights for all retrodicted scans. It is found, however, that retrodiction more than $\simeq 6$ scans backward does not improve the track smoothness, i.e. older track history may be fixed without drawbacks.

2.6 Coordinate Transformation

The incoming GMTI-data are given in the *World Geodetic System 84* (WGS84) format [8], whereas the tracking system works in local two dimensional cartesian coordinates. Hence the GMTI-measurements are transformed using the following formulas:

$$\begin{aligned}
\Delta L &= L_{\text{reference}} - L_{\text{GMTI}}\\
\Delta B &= B_{\text{reference}} - B_{\text{GMTI}}\,,
\end{aligned}$$

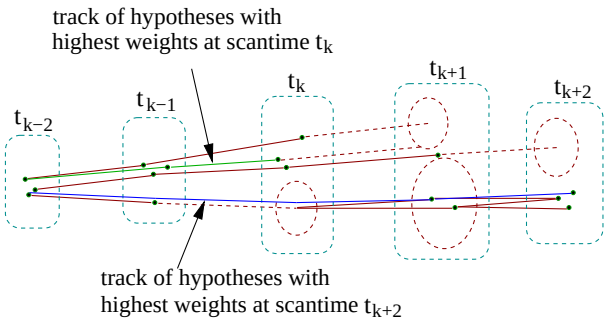

Figure 3: Switching event of the MHT-subtrack with highest weight caused by retrodiction

where L means the longitude and B the latitude of the considered coordinate. With this difference coordinates, the local coordinates are given as

$$\begin{aligned}
X_{\text{local}} = \Delta X &= N(B_{\text{reference}})\cos B_{\text{reference}}\,\Delta L\\
Y_{\text{local}} = \Delta Y &= M(B_{\text{reference}})\Delta B
\end{aligned}$$

with

$$M(B) = \frac{a(1-e^2)}{(1-e^2\sin^2 B)^{\frac{3}{2}}} \quad \text{and} \quad N(B) = \frac{a}{\sqrt{1-e^2\sin^2 B}}$$

whereas $a = 6378137.0$ m and $e^2 \simeq 6.69438 \cdot 10^{-3}$ given by the definition of the WGS84 ellipsoid. The backward transformation may also be easily carried out.

3 EXPERIMENTAL RESULTS

We present tracking results for simulated GMTI sensor data generated from a ground truth of a Kosovo scenario produced at the NC3A for the simulation experiments SIMEX2003 and TIE2004 in Den Haag.

Recently, the IIES with the experimental tracking component took part in a technical integration exercise (TIE2004) at the NC3A in Den Haag. The test plan for TIE 2004 covered several issues concerning the compliance and technical interoperability of the multi-national system. Test objectives, among others, were: compliance with NATO STANAGs, access mechanisms for data dissemination, distributed simulation, MTI exploitation, and track management. The participating SAR and GMTI sensor simulators were:

1. Airborne Stand-Off Radar (ASTOR), GB
2. Complesso Radar Eliportato di Sorveglianca (CRESO), IT
3. Hélicoptère d'Observation Radar et d'Investigation sur Zone (HORIZON), FR

4. Global Hawk, US
5. Radarsat 2, CA
6. U2-AIP, US
7. Virtual Joint Surveillance and Target Attack Radar System (VSTARS), US

The sensor data were disseminated over an Exploitation (EX) LAN to various exploitation stations and other C2 systems. In both online and offline modes the access to the database is provided by CORBA APIs. For visualization and interactive processing, the data are send to several *human computer interfaces (HCI)*. The MTI data are also fed into the tracking module which delivers, also via CORBA APIs, relevant track information back to the data base and eventually to the visualization and a track management HCI. The architecture of the German ground station IIES including the tracker integration is sketched in Fig. 4. Besides the U2 and Radarsat sensors, tracks could be extracted from data of all sensors. In the former cases, the observation times and number of scans in a given surveillance region were too short to establish meaningful tracks. For the other sensors, a mission typically consists of 100–400 scans, separated by a time interval of about 5–30 sec. The number of MTI detection per scan ranges from zero to a few hundred. Depending on the data quality, it takes usually 3-4 scans to confirm a track. The false alarm density is estimated about $p_f = 0.1\text{km}^2$, and the detection probability $P_D = 0.9$. Since the existing MTI DOPPLER measurements often prove not reliable they are not taken into account for the tracking. Even for large area scans with many MTI detections, the performance of the tracking module is close to real time. Here, we present some exemplary tracking results from a generic sensor simulator. More detailed results for specific simulated GMTI sensor data as well as for real HORIZON data from the NATO live exercise *Strong Resolve* (Norway, March 2002) can be found in [9]. Figure 5 depicts the tracks of two groups of road targets, one of it is leaving the road in the second snapshot. Figure 6 shows a track of a target with several missing detections. The displacement between road and track is due to road map errors. Figure 7, finally, shows tracking results generated from the measurements of simulated railway traffic.

While these first tracking results are quite encouraging, there is still a lot room for improvements:

1. Targets with strongly different speed and agility are difficult to track within a single target dynamics model.
2. The clutter density often is strongly inhomogeneous leading to unsuitable model parameters in parts of the surveillance region.
3. Track continuity is hard to establish in case of dense road traffic.

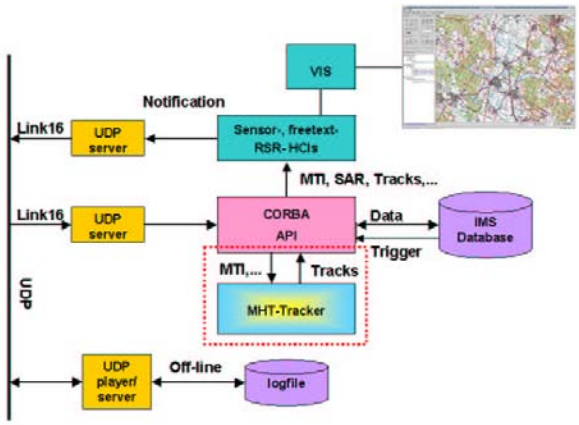

Figure 4: Scheme of the architecture of the exploitation station IIES including the MHT-tracking module.

4. For target aggregations, e.g. convoys, target number estimation is desirable.
5. Extended targets (e.g. trains, ships and ferries) provide a *detection cloud*, in particular in case of high sensor resolution. Here, estimates of the center of mass and target extension are desirable.

For all of these issues, there exist suitable approaches which can be integrated step by step into the MHT tracking algorithm. [10, 11, 12, 13, 14]

4 CONCLUSION AND OUTLOOK

We have presented techniques and algorithms for track extraction and track maintenance for GMTI sensor data. The method at choice is a multi hypothesis tracker which performs both tasks simultaneously. The algorithm is adapted to the case of ground targets and has been integrated into the German experimental MTI and SAR exploitation station IIES. Tracking results using real data from the NATO exercise Strong Resolve 2002 [9] and from simulated reconnaissance missions demonstrate successful tracking of a number of different ground, sea, and low flying targets in a large area, partly with high clutter density. The performance is close to real time, even for relatively large target numbers and high clutter. For a quantitative evaluation of track precision and track continuity, the additional knowledge of the ground truth of relevant targets is necessary. Such information will be available in the near future for real data from a flight campaign of the experimental SAR/MTI system PAMIR (*Phased Array Multifunctional Imaging Radar*) developed at FGAN/FHR. [15, 16]

Further improvements of the algorithm will include:

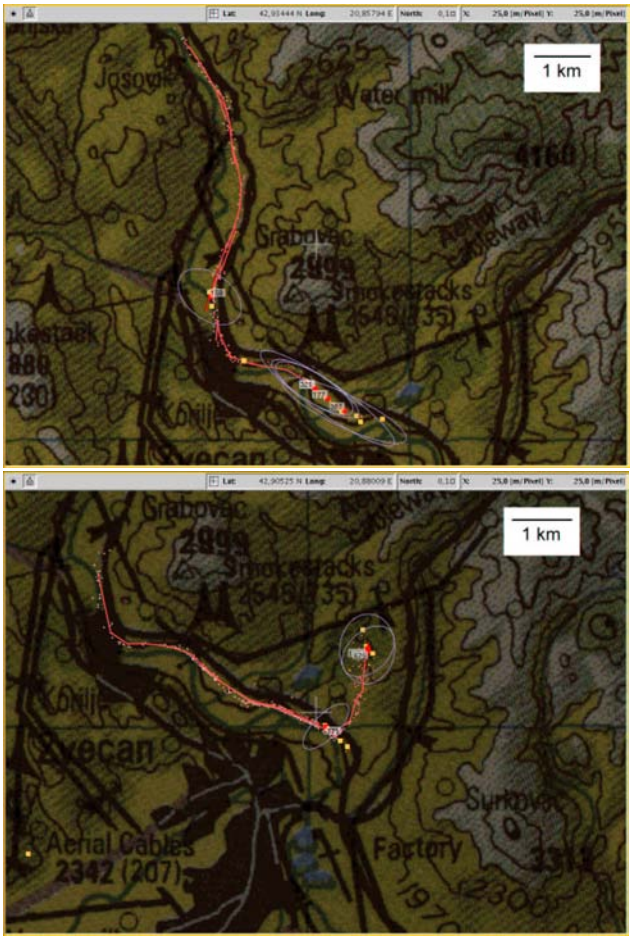

Figure 5: Above: MH Tracks of two target groups with model parameters (v_t=20 m/s, θ_t=60 s) leads to reasonable tracks near the roads. Bottom: The same track some scans later. Error ellipses correspond to a 99.9% convidence level (3.3σ).

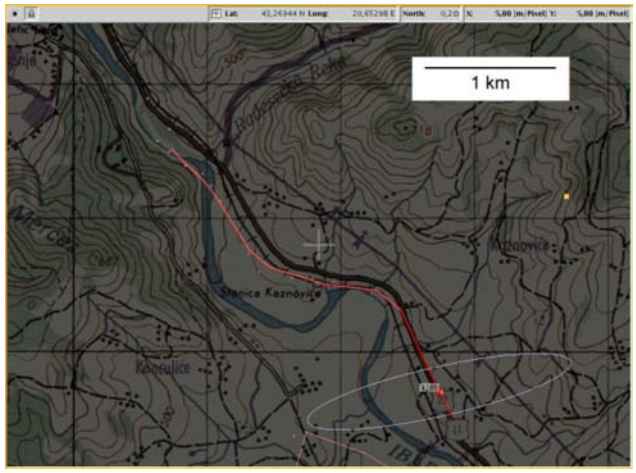

Figure 6: Single road target with sparse measurements

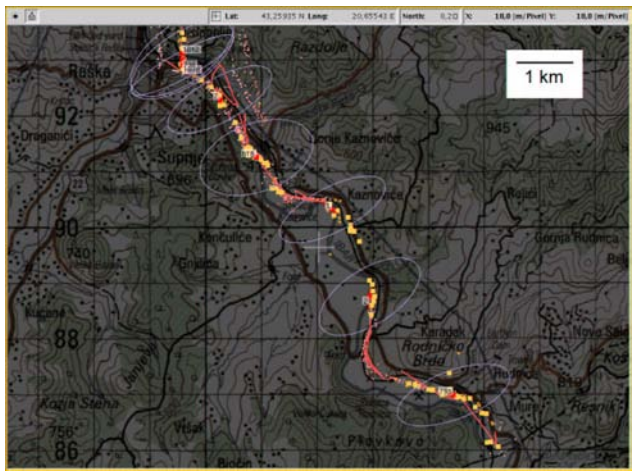

Figure 7: Tracks of several railway targets.

1. Use of road-map and terrain visibility information provided by topographic maps [17]
2. Realistic modeling of the *clutter notch* of the MTI sensors [12, 18]
3. Multiple model approach for different target types
4. Use of *Doppler* measurements and attribute information provided by the sensor
5. Target number detection in case of target aggregations

Acknowledgment

The authors wish to thank W. Koch for helpful discussions and suggestions, H. Bös for the implementation of the IIES–tracker interfaces, R. Beck and M. Karremann (M4COM) for supporting the integration into the IIES and the NC3A for providing simulation data and testbed infrastructure.

References

[1] R. Klemm, *Space-time adaptive processing - principles and applications*. IEE Publishers, 1998.

[2] S. Blackman and R. Popoli, *Design and Analysis of Modern Tracking Systems*. Artech House, Boston MA, 1999.

[3] Y. Bar-Shalom and X.-R. Li, *Estimation and Tracking: Principles, Techniques, and Software*. Boston MA: Artech House, 1993.

[4] G. v. Keuk, "Sequential track extraction," *IEEE Transaction on Aerospace and Electronic Systems*, vol. 34, pp. 1135–1148, 1998.

[5] X. R. Li and V. P. Jilkov, "A survey of maneuvering target tracking dynamical models," in *Proc. of Signal and Data Processing of Small Targets* (O. E. Drummond, ed.), vol. 4048, p. 212, SPIE, 2000.

[6] We define: $\mathcal{N}(\mathbf{x}; \mathbf{x_0}, \mathbf{P}) \equiv [\det(2\pi\mathbf{P})]^{-1/2} \exp[-\frac{1}{2}(\mathbf{x}-\mathbf{x_0})^\top \mathbf{P}^{-1}(\mathbf{x}-\mathbf{x_0})]$.

[7] A. Wald, *Sequential Analysis*. John Wiley, New York, 1947.

[8] "World Geodetic System 84." http://www.wgs84.com.

[9] J. Koller, H. B"os, and M. Ulmke, "Track extraction and multi hypothesis tracking for GMTI sensor data." FKIE-Bericht Nr. 90, FGAN e.V. (Wachtberg), 2005.

[10] K. Kastella, C. Kreucher, and M. A. Pagels, "Nonlinear filtering for ground target applications," in *Proc. of Signal and Data Processing of Small Targets* (O. E. Drummond, ed.), vol. 4048, pp. 266–276, SPIE, 2000.

[11] T. Kirubarajan, Y. Bar-Shalom, and K. R. Pattipati, "Topography-based VS-IMM estimator for large-scale ground target tracking," in *IEE Colloquium on Target Tracking: Algorithms and Applications*, pp. 11/1 –11/4, 1999.

[12] W. Koch, "GMTI-tracking and information fusion for ground surveillance," in *Proc. of Signal and Data Processing of Small Targets* (O. E. Drummond, ed.), vol. 4473, p. 381, SPIE, 2001.

[13] W. Koch, "On Expectation Maximization applied to GMTI convoy tracking," in *Proc. of Signal and Data Processing of Small Targets* (O. E. Drummond, ed.), (Orlando), SPIE, April 2002. to appear.

[14] W. Koch, "Information Fusion aspects related to GMTI convoy tracking," in *Proc. Int. Conf. Information Fusion*, (Annapolis), pp. 1038–1045, ISIF, July 2002.

[15] J. Ender and A. Brenner, "PAMIR - a wideband phased array SAR/MTI system," in *IEE Proc.-Radar Sonar Navigation*, vol. 150, pp. 165–172, 2003.

[16] D. Cerutti-Maori and U. Skupin, "First experimental SCAN/MTI results achieved with the multi-channel SAR-system PAMIR," in *Proceedings of the 5th European Conference on Synthetic Aperture Radar EuSAR*, vol. 2, pp. 521–524, may 2004.

[17] M. Ulmke, "Improved GMTI-tracking using roadmaps and topographic information," in *Proc. of Signal and Data Processing of Small Targets* (O. E. Drummond, ed.), vol. 5204, SPIE, 2003.

[18] W. Koch and R. Klemm, "Ground target tracking with STAP radar," in *IEE Proc.-Radar, Sonar Navig.*, vol. 148, pp. 173–185, IEE, 2001.